ARTICLE

OBC
www.rsc.org/obc

Cyclodextrin and modified cyclodextrin complexes of *E*-4-*tert*-butylphenyl-4′-oxyazobenzene: UV-visible, ^{1}H NMR and *ab initio* studies†

Bruce L. May,[a] Jacobus Gerber,[a] Philip Clements,[a] Mark A. Buntine,[a] David R. B. Brittain,[a] Stephen F. Lincoln*[a] and Christopher J. Easton[b]

[a] *Department of Chemistry, University of Adelaide, Adelaide, SA 5005, Australia. E-mail: Stephen.Lincoln@adelaide.edu.au*

[b] *Research School of Chemistry, Australian National University, Canberra, ACT 0200, Australia*

Received 8th October 2004, Accepted 2nd February 2005
First published as an Advance Article on the web 11th March 2005

α-Cyclodextrin, β-cyclodextrin, *N*-(6^A-deoxy-α-cyclodextrin-6^A-yl)-*N*′-(6^A-deoxy-β-cyclodextrin-6^A-yl)urea and *N*,*N*-bis(6^A-deoxy-β-cyclodextrin-6^A-yl)urea (αCD, βCD, **1** and **2**) form inclusion complexes with *E*-4-*tert*-butylphenyl-4′-oxyazobenzene, *E*-**3**$^-$. In aqueous solution at pH 10.0, 298.2 K and $I = 0.10$ mol dm^{-3} ($NaClO_4$) spectrophotometric UV-visible studies yield the sequential formation constants: $K_{11} = (2.83 \pm 0.28) \times 10^5$ dm^3 mol^{-1} for αCD·*E*-**3**$^-$, $K_{21} = (6.93 \pm 0.06) \times 10^3$ dm^3 mol^{-1} for (αCD)$_2$·*E*-**3**$^-$, $K_{11} = (1.24 \pm 0.12) \times 10^5$ dm^3 mol^{-1} for βCD·*E*-**3**$^-$, $K_{21} = (1.22 \pm 0.06) \times 10^4$ dm^3 mol^{-1} for (βCD)$_2$·*E*-**3**$^-$, $K_{11} = (3.08 \pm 0.03) \times 10^5$ dm^3 mol^{-1} for **1**·*E*-**3**$^-$, $K_{11} = (8.05 \pm 0.63) \times 10^4$ dm^3 mol^{-1} for **2**·*E*-**3**$^-$ and $K_{12} = (2.42 \pm 0.53) \times 10^4$ dm^3 mol^{-1} for **2**·(*E*-**3**$^-$)$_2$. ^{1}H ROESY NMR studies show that complexation of *E*-**3**$^-$ in the annuli of αCD, βCD, **1** and **2** occurs. A variable-temperature ^{1}H NMR study yields k(298 K) = 6.7 ± 0.5 and 5.7 ± 0.5 s^{-1}, $\Delta H^{\ddagger} = 61.7 \pm 2.7$ and 88.1 ± 4.2 kJ mol^{-1} and $\Delta S^{\ddagger} = -22.2 \pm 8.7$ and 65 ± 13 J K^{-1} mol^{-1} for the interconversion of the dominant includomers (complexes with different orientations of αCD) of αCD·*E*-**3**$^-$ and (αCD)$_2$·*E*-**3**$^-$, respectively. The existence of *E*-**3**$^-$ as the sole isomer was investigated through an *ab initio* study.

Introduction

The aim of this study is to improve insight into the structural and mechanistic factors controlling the formation of cyclodextrin (CD) and linked CD dimer inclusion complexes. The significance of the linked CD dimers is that CDs are linked together so that their simultaneous complexation of a guest species may be varied as the sizes of the CD annuli are changed. We have chosen to study the interactions of αCD and βCD separately and as components of *N*-(6^A-deoxy-α-cyclodextrin-6^A-yl)-*N*′-(6^A-deoxy-β-cyclodextrin-6^A-yl)urea[1] (**1**) and *N*,*N*-bis(6^A-deoxy-β-cyclodextrin-6^A-yl)urea[2] (**2**) with *E*-4-*tert*-butyl-4′-oxyazobenzene (*E*-**3**$^-$) (Scheme 1) through the complexes αCD·*E*-**3**$^-$, (αCD)$_2$·*E*-**3**$^-$, βCD·*E*-**3**$^-$, (βCD)$_2$·*E*-**3**$^-$, **1**·*E*-**3**$^-$, **2**·*E*-**3**$^-$ and **2**·(*E*-**3**$^-$)$_2$. While the effects of the difference in annular size of αCD and βCD on complex stoichiometry and stability have been widely studied[3,4] their impact on complexation by linked CDs, exemplified by **1** and **2**, is less explored,[1,5,6] as are their effects on rate processes exemplified by the exchange between the includomers (complexes with different orientations of αCD) of αCD·*E*-**3**$^-$ and (αCD)$_2$·*E*-**3**$^-$ reported here. The choice of *E*-**3**$^-$ is based on it possessing a large hydrophobic 4-*tert*-butylphenyl group which discriminates between the annular sizes of αCD and βCD and a smaller and less hydrophobic 4′-oxybenzene group which discriminates to a lesser extent. In contrast to the azobenzenes which exist in thermally and photochemically controlled equilibria of their *E* and *Z* isomers,[7–10] only *E*-**3**$^-$ was observed under the conditions of this study. *Ab initio* modelling[11] has been undertaken to gain insight into the existence of *E*-**3**$^-$ as the sole isomer.

Results and discussion

UV-visible spectroscopic studies

The parent guest species *E*-4-*tert*-butylphenyl-4′-hydroxyazobenzene, *E*-**3**H, and its CD complexes are insufficiently water soluble for convenient study. As a consequence the much more soluble *E*-4-*tert*-butylphenyl-4′-oxyazobenzene, *E*-**3**$^-$, and its CD and CD dimer complexes were studied at 298.2 K in aqueous 0.05 mol dm^{-3} borate buffer at pH 10 and $I = 0.10$ mol dm^{-3} ($NaClO_4$). The variations of the molar absorbance of *E*-**3**$^-$ with αCD, βCD, **1** and **2** concentrations are shown in Figs. 1–3 and Figs. S1–S5, ESI,† and the derived complexation constants appear in Table 1. Complexation by αCD causes a much greater molar absorbance change than does βCD consistent with the smaller size of the αCD annulus producing a greater change in the environment of *E*-**3**$^-$ (Figs. 1 and 2, Figs. S1 and S2, ESI†). Both αCD·*E*-**3**$^-$ and (αCD)$_2$·*E*-**3**$^-$ are formed as are their βCD analogues. In addition to the statistical effect on the relative magnitudes of sequential complexation constants, the differences in hydrophobicity and size between the two ends of *E*-**3**$^-$ accentuate the difference in the magnitudes of K_{11} and K_{21} (Table 1).

The two isosbestic points seen in the molar absorbance variation of *E*-**3**$^-$ with [**1**]$_{total}$ (Fig. 3 and Fig. S3, ESI†) are consistent with *E*-**3**$^-$ and **1**·*E*-**3**$^-$ being the dominant species in solution whereas the spectral variation of *E*-**3**$^-$ with [**2**]$_{total}$ (Figs. S4 and S5, ESI†) is consistent with the formation of **2**·*E*-**3**$^-$ and **2**·(*E*-**3**$^-$)$_2$ as shown in Scheme 2 wherein αCD and βCD are shown as truncated cones where the narrow ends represent the primary hydroxy ends of the annuli. Despite the linking of αCD and βCD in **1** and **2** there is little cooperativity between them in complexing *E*-**3**$^-$ in **1**·*E*-**3**$^-$ and **2**·*E*-**3**$^-$ as shown by the similarity of their K_{11} values to those of αCD·*E*-**3**$^-$ and βCD·*E*-**3**$^-$. (This contrasts with the complexation of the Methyl Orange anion by βCD and **2** for which $K_{11} = 2.16 \times 10^3$

† Electronic supplementary information (ESI) available: UV-vis spectra and data, NMR spectra and *ab initio* figures and discussion. See http://www.rsc.org/suppdata/ob/b4/b415594g/

DOI: 10.1039/b415594g

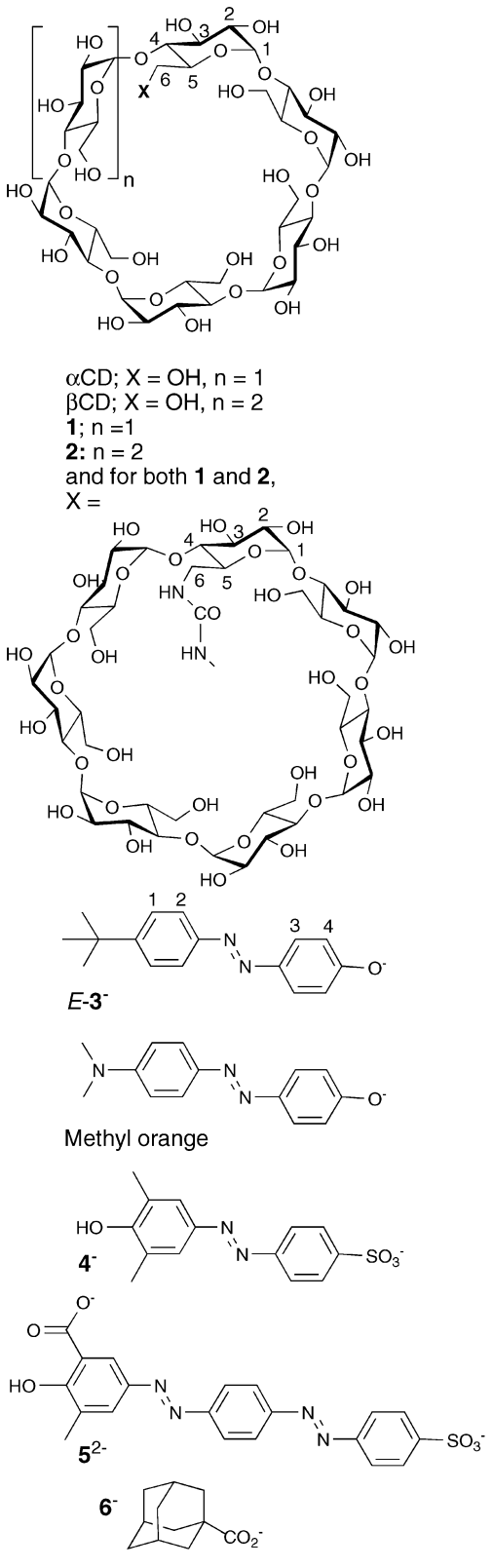

Scheme 1

and 1.05×10^5 dm^3 mol^{-1}, respectively, despite the structural similarity of this anion and *E*-**3**$^-$as shown in Scheme 1.[5]) The four systems show a variation of only a factor of 3.8 in K_{11} for αCD·*E*-**3**$^-$, βCD·*E*-**3**$^-$, **1**·*E*-**3**$^-$ and **2**·*E*-**3**$^-$. The complexation of a second *E*-**3**$^-$ in **2**·(*E*-**3**$^-$)$_2$ is characterised by K_{12} which is only a factor of 3.3 less than K_{11} for **2**·*E*-**3**$^-$. It appears that the hydrophobic 4-*tert*-butylphenyl groups of the two *E*-**3**$^-$ are complexed in each βCD component annulus of **2**. This is consistent with the analogous **1**·(*E*-**3**$^-$)$_2$ complex not forming at detectable levels probably because the αCD annulus is too small to accommodate the 4-*tert*-butylphenyl group of *E*-**3**$^-$ and complexation of the charged 4′-oxybenzene group is weaker such that the formation of **1**·(*E*-**3**$^-$)$_2$ does

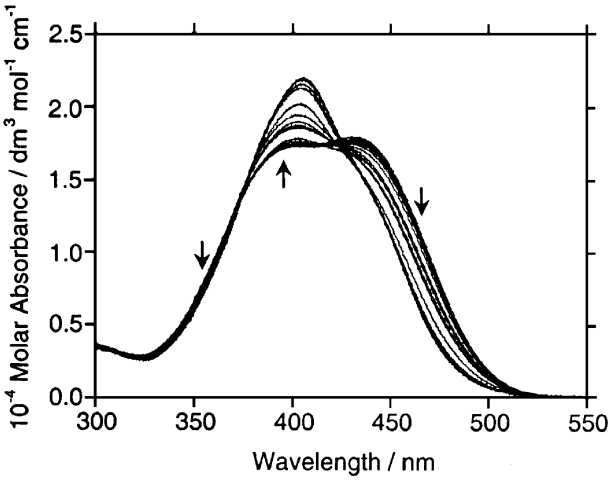

Fig. 1 The change in the UV-visible molar absorbance of *E*-**3**$^-$ (indicated by arrows) with increase in $[\alpha CD]_{total}$ in aqueous borate buffer solution at pH 10.0, 298.2 K and $I = 0.10$ mol dm^{-3} ($NaClO_4$); $[E\text{-}\mathbf{3}^-]_{total} = 1.92 \times 10^{-5}$ mol dm^{-3} and $[\alpha CD]_{total} = 1.20 \times 10^{-6}$–$1.20 \times 10^{-3}$ mol dm^{-3}.

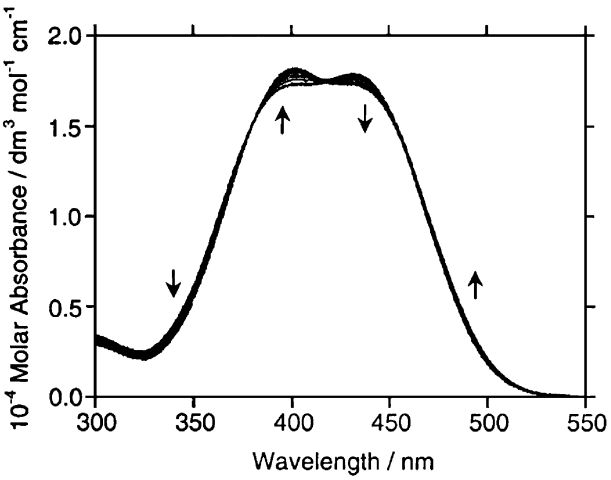

Fig. 2 The change in the UV-visible absorbance of *E*-**3**$^-$ (indicated by arrows) with increase in $[\beta CD]_{total}$ in aqueous borate buffer solution at pH 10.0, 298.2 K and $I = 0.10$ mol dm^{-3} ($NaClO_4$): $[E\text{-}\mathbf{3}^-]_{total} = 1.86 \times 10^{-5}$ mol dm^{-3} and $[\beta CD]_{total} = 1.22 \times 10^{-6}$–$1.22 \times 10^{-3}$ mol dm^{-3}.

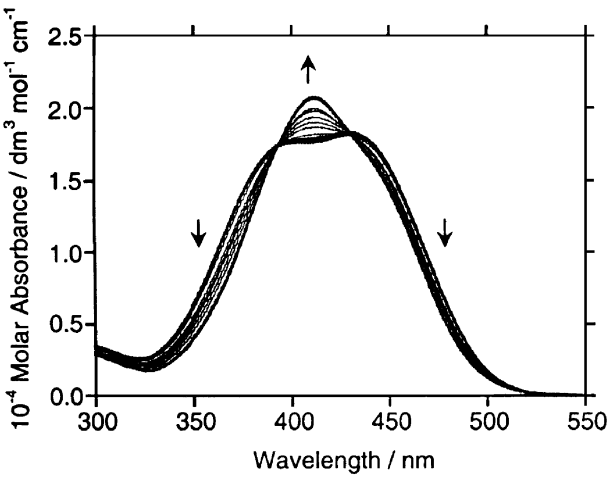

Fig. 3 The change in the UV-visible absorbance of *E*-**3**$^-$ (indicated by arrows) with increase in $[\mathbf{1}]_{total}$ in aqueous borate buffer solution at pH 10.0, 298.2 K and $I = 0.10$ mol dm^{-3} ($NaClO_4$); $[E\text{-}\mathbf{3}^-]_{total} = 1.92 \times 10^{-5}$ mol dm^{-3} and $[\mathbf{1}]_{total} = 2.28 \times 10^{-7}$–$2.28 \times 10^{-4}$ mol dm^{-3}. Isosbestic points occur at 394 and 430 nm.

Table 1 Sequential complexation constants determined in aqueous borate buffer (0.05 mol dm^{-3}) at pH 10, $I = 0.10$ mol dm^{-3} ($NaClO_4$) and 298.2 K

Complex	K_{11}/dm^3 mol^{-1}	K_{21}/dm^3 mol^{-1}	K_{12}/dm^3 mol^{-1}
αCD·*E*-**3**$^-$	$(2.83 \pm 0.28) \times 10^5$		
(αCD)$_2$·*E*-**3**$^-$		$(6.93 \pm 0.06) \times 10^3$	
βCD·*E*-**3**$^-$	$(1.24 \pm 0.12) \times 10^5$		
(βCD)$_2$·*E*-**3**$^-$		$(1.22 \pm 0.06) \times 10^4$	
1·*E*-**3**$^-$	$(3.08 \pm 0.03) \times 10^5$		
2·*E*-**3**$^-$	$(8.05 \pm 0.63) \times 10^4$		
2·(*E*-**3**$^-$)$_2$			$(2.42 \pm 0.53) \times 10^4$

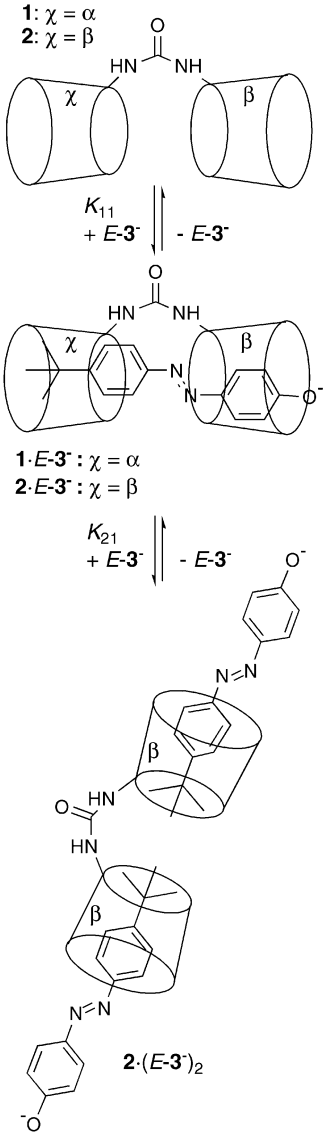

Scheme 2

not compete effectively with the formation of **1**·*E*-**3**$^-$. This infers significant stereochemical differences in the complexing of *E*-**3**$^-$ by either αCD or βCD alone or as components of **1** and **2**, as is supported by the ^{1}H NMR studies discussed below. Nevertheless, all of the complexes exhibit high stabilities within the general range of CD complex stabilities.

^{1}H NMR complexation studies of αCD and βCD complexes

The ^{1}H NMR spectra of *E*-**3**$^-$ and its CD complexes were run at higher concentrations than those used in the UV-vis studies. To achieve these concentrations it was necessary to prepare all solutions in D_2O from *E*-**3**H and the chosen CD or CD dimer in 0.10 mol dm^{-3} NaOD such that pD ≈ 12. This may indicate that it is necessary to deprotonate a CD hydroxy group (which is expected to have a p$K_a \geq 12$ on the basis that the pK_as of OH(2) and OH(3) are 12.33 for αCD[4]) to achieve the required solubility. (In the absence of a CD, *E*-**3**$^-$ has a very low solubility under these conditions.) Despite this, the stoichiometry of the CD complexes formed appeared to correspond to those detected in the UV-vis studies.

In the ^{1}H NMR spectrum of an equimolar solution of *E*-**3**$^-$ and αCD the *tert*-butyl resonance appears as two singlets and the *E*-**3**$^-$ aromatic H1–4 doublets arising from AA′BB′ spin–spin splitting are duplicated, consistent with the formation of αCD·*E*-**3**$^-$ as two includomers, A and B (Scheme 3). The ^{1}H ROESY NMR spectrum of αCD·*E*-**3**$^-$ (Fig. 4) shows strong cross-peaks between the H1–3 resonances of *E*-**3**$^-$ and those of the αCD

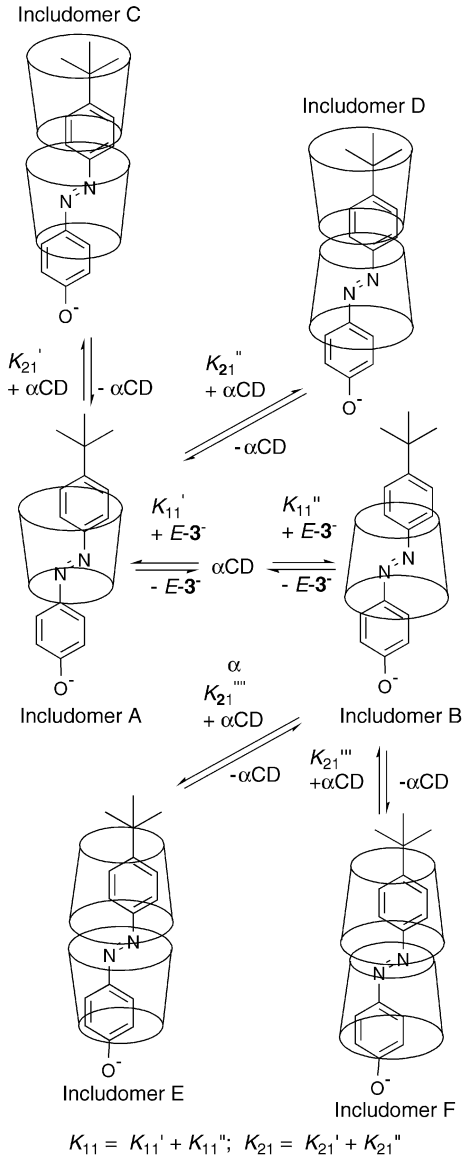

Scheme 3

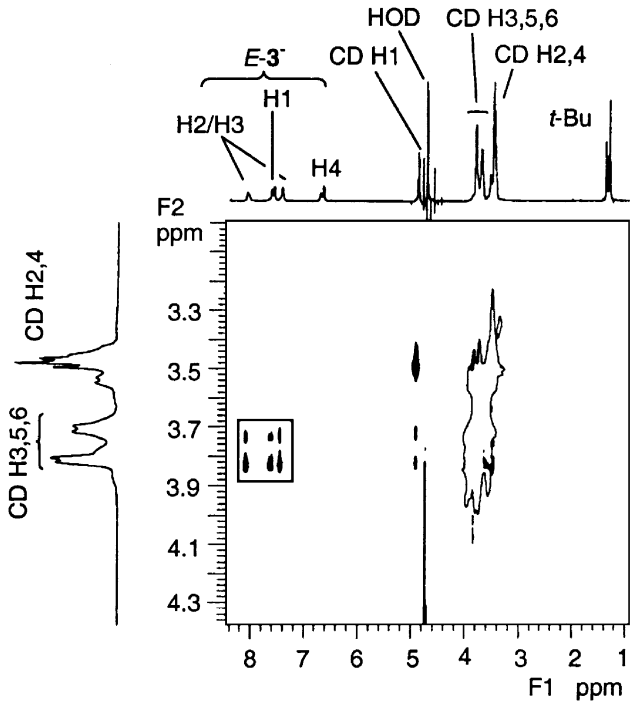

Fig. 4 ^{1}H 600 MHz ROESY NMR spectrum of 0.01 mol dm^{-3} αCD and *E*-**3**$^-$ which exist dominantly as αCD·E-**3**$^-$ in 0.10 mol dm^{-3} NaOD at 298 K. The cross-peaks enclosed in the rectangles correspond to NOE interactions between the protons indicated on the F1 and F2 axes.

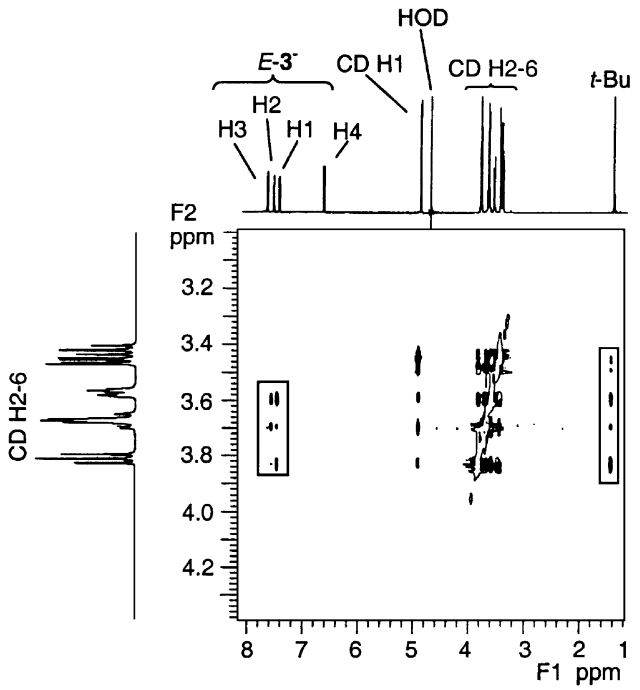

Fig. 5 ^{1}H 600 MHz ROESY NMR spectrum of 0.01 mol dm^{-3} βCD and *E*-**3**$^-$, which exist dominantly as βCD·*E*-**3**$^-$ in 0.10 mol dm^{-3} NaOD at 298 K. The cross-peaks enclosed in the rectangles correspond to NOE interactions between the protons indicated on the F1 and F2 axes.

3H, 5H and 6H protons of the annular interior. No cross-peaks are observed for the *tert*-butyl protons and the αCD protons consistent with the *tert*-butyl group residing in the vicinity of either the primary or secondary hydroxy ring of αCD. These observations suggest that in both αCD·*E*-**3**$^-$ includomers αCD is positioned over the diazo bond of *E*-**3**$^-$ such that protons H1–3 are closest to the interior of the αCD annulus. Although the *tert*-butyl protons are insufficiently close to the interior of the αCD annulus to generate cross-peaks, the magnetic environments of the includomers A and B are sufficiently different to produce two *tert*-butyl resonances. These observations may indicate that αCD is sterically hindered from interacting with the *tert*-butyl group of *E*-**3**$^-$ in αCD·*E*-**3**$^-$. This interpretation is supported by the observation of strong *tert*-butyl and H1 and H2 *E*-**3**$^-$ cross-peaks in the ^{1}H ROESY NMR spectrum of βCD·*E*-**3**$^-$ (Fig. 5) which indicates that the *tert*-butyl protons are within ~4 Å of the βCD annular H3, 5 and 6 protons consistent with the larger βCD annulus more readily accommodating the 4-*tert*-butylphenyl group. The *tert*-butyl and H1–H4 *E*-**3**$^-$ resonances of βCD·*E*-**3**$^-$ appear as a sharp singlet and well resolved doublets, respectively, consistent with βCD·*E*-**3**$^-$ existing as either a single includomer or two includomers in fast exchange. This deduction is supported by the βCD resonances being much better resolved for βCD·*E*-**3**$^-$ than is the case for αCD in αCD·*E*-**3**$^-$.

The two *tert*-butyl ^{1}H resonances of αCD·*E*-**3**$^-$ appear in the area ratio 2.86 : 1 at 298 K consistent with includomers A and B of αCD·*E*-**3**$^-$ existing in the same ratio and $\Delta H^0 = 11.4 \pm 2.6$ kJ mol^{-1} and $\Delta S^0 = 47.0 \pm 8.4$ J K^{-1} mol^{-1} derived from the kinetic parameters characterizing the interconversion of the two includomers (Fig. 6). The same ratio is also shown by the duplicated aromatic doublet resonances of αCD·*E*-**3**$^-$ (Fig. S6, ESI†). The assignment of these resonances to specific includomers can not be made with certainty. As temperature increases, the pair of *tert*-butyl resonances broaden and coalesce and complete lineshape analysis[12,13] in the range 298–318 K yields the kinetic parameters in Table 2, where k_A and k_B are the decomplexation rate constants for includomers A and B, respectively, and $k_A X_A = k_B X_B$ where X_A and X_B are the corresponding mole fractions. Interconversion probably occurs

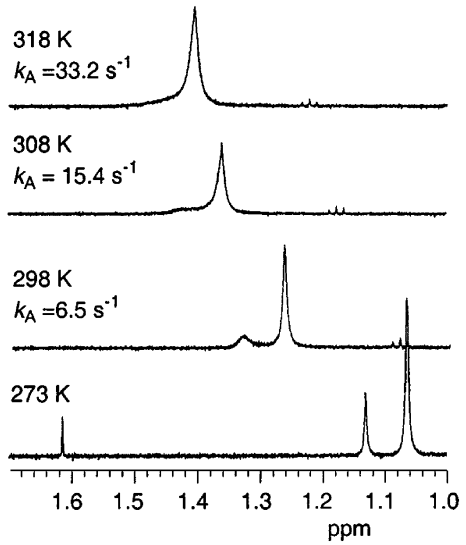

Fig. 6 Representative variable-temperature ^{1}H 600 MHz NMR spectra of the *tert*-butyl protons of *E*-**3**$^-$ in αCD·*E*-**3**$^-$ showing k_A at each temperature (k_A = 10.4 s^{-1} at 303 K and 23.7 at 313 K; k_B = 18.7, 32.2, 51.3, 84.6 and 127 s^{-1} at 298, 303, 308, 313 and 318 K, respectively.) The spectra are not plotted to a constant vertical scale. The solution is 0.01 mol dm^{-3} in αCD and *E*-**3**$^-$ in 0.10 mol dm^{-3} NaOD.

through decomplexation of the αCD·*E*-**3**$^-$ includomer A to αCD and *E*-**3**$^-$ followed by the formation of αCD·*E*-**3**$^-$ includomer B. Under these circumstances, $k_{A*}/k_A = K_{11}'$ and $k_{B*}/k_B = K_{11}''$ where k_{A*} and k_{B*} are the second-order rate constants for the formation of includomers A and B, respectively. In principle, the addition of a second αCD to form (αCD)$_2$·*E*-**3**$^-$ followed by the dissociation of an αCD to give αCD·*E*-**3**$^-$ provides an alternative path for interconversion. However, as it appears that the αCD annulus is too small to readily pass over the 4-*tert*-butylphenyl group of *E*-**3**$^-$, this second mechanism seems less likely. If it is assumed that the 4′-oxybenzene group of *E*-**3**$^-$ more easily enters the wide end of the αCD annulus than it does the narrow end, the dominant includomer is A. The negative sign of $\Delta S_A^{\ddagger}$ for the decomplexation of includomer A reflects an increase in order as

Table 2 Kinetic parameters for interconversion of includomers and decomplexation

Complex	k(298 K)/s^{-1}	$\Delta H^{\ddagger}$/kJ mol^{-1}	$\Delta S^{\ddagger}$/J K^{-1} mol^{-1}
αCD·*E*-**3**$^-$ includomer A	6.7 ± 0.5 (k_A)	61.7 ± 2.7	−22.2 ± 8.7
αCD·*E*-**3**$^-$ includomer B	19.2 ± 1.5 (k_B)	73.1 ± 2.7	24.8 ± 8.7
(αCD)$_2$·*E*-**3**$^-$ includomer C	5.7 ± 0.5 (k_C)	88.1 ± 4.2	65 ± 13
(αCD)$_2$·*E*-**3**$^-$ includomer D	14.7 ± 0.5 (k_D)	79.2 ± 4.2	43 ± 13
αCD·**4**$^-$ [a]	13.3	44.6	−73.9
αCD·**4**$^-$ [a]	0.22	47.5	−98.3
αCD·**5**$^{2-}$ [b]	4.4	49.7	−67
(αCD)$_2$·**5**$^{2-}$ [b]	0.032	60.1	−76

[a] Ref. 14. [b] Ref. 16.

the transition state is reached whereas the opposite applies for includomer B as is discussed below.

The ^{1}H ROESY NMR spectrum of a solution in which the mole ratio of *E*-**3**$^-$ and αCD was 1 : 3 shows cross-peaks between the H1–3 and *tert*-butyl protons of *E*-**3**$^-$ and the H3, H5 and H6 protons of αCD but no analogous cross-peaks for H4 of *E*-**3**$^-$ (Fig. 7). This is consistent with the formation of (αCD)$_2$·*E*-**3**$^-$ (Scheme 3) in which one αCD envelopes the *tert*-butyl group of *E*-**3**$^-$ and part of the adjacent phenyl group while the second αCD is positioned partly over the diazo bond and part of both phenyl rings with H4 of *E*-**3**$^-$ being too distant to generate cross-peaks with αCD H3, H5 and H6. This disposition of the two αCD in (αCD)$_2$·*E*-**3**$^-$ is probably aided by the 4-*tert*-butylphenyl group of *E*-**3**$^-$ being strongly hydrophobic whereas the 4′-oxybenzene group is less so. The *tert*-butyl resonance is split into two singlets and each of the *E*-**3**$^-$ H3, H5 and H6 doublets are split into two doublets consistent with (αCD)$_2$·*E*-**3**$^-$ existing as two includomers. However, the observations on the αCD·*E*-**3**$^-$ includomers are consistent with the 4-*tert*-butylphenyl group of *E*-**3**$^-$ only being enveloped by the wider end of αCD under the influence of increased steric crowding as a second αCD complexes *E*-**3**$^-$ in (αCD)$_2$·*E*-**3**$^-$. Thus, the structures of the two includomers of (αCD)$_2$·*E*-**3**$^-$ (C and D) are probably as shown in Scheme 2, and may only form from the αCD·*E*-**3**$^-$ A includomer. Consequently, interconversion between the C and D includomers of (αCD)$_2$·*E*-**3**$^-$ occurs through decomplexation of the αCD adjacent to the 4′-oxybenzene group of *E*-**3**$^-$ followed by complexation of another αCD in the opposite orientation. By this reasoning, the E and F includomers (αCD)$_2$·*E*-**3**$^-$ (Scheme 3) are likely to be relatively unstable because the narrow end of the αCD annulus envelopes less of the 4-*tert*-butylphenyl group of *E*-**3**$^-$ in the E and F includomers than is the case for the C and D includomers, and the second αCD is thereby more hindered in its complexation of *E*-**3**$^-$. The ^{1}H ROESY NMR spectrum of (βCD)$_2$·*E*-**3**$^-$ shows cross-peaks between the H1–3 and *tert*-butyl protons of *E*-**3**$^-$ and the H3, H5 and H6 protons of βCD but no cross-peaks for H4 of *E*-**3**$^-$. This spectrum is similar to that observed for βCD·*E*-**3**$^-$ in that both the βCD and *E*-**3**$^-$ resonances are much better resolved than are the αCD and *E*-**3**$^-$ resonances of (αCD)$_2$·*E*-**3**$^-$ (Fig. S7, ESI†).

The two singlets observed for the *tert*-butyl group and pairs of doublets H2, H3 and H4 of *E*-**3**$^-$ in (αCD)$_2$·*E*-**3**$^-$ exist in the area ratio 2.46 : 1 at 305 K consistent with two includomers (C and D) of (αCD)$_2$·*E*-**3**$^-$ existing in the same ratio (Fig. 8). This ratio diminishes with increasing temperature and ΔH° = 8.90 ± 0.43 kJ mol^{-1} and ΔS^{0} = 21.9 ± 1.4 J K^{-1} mol^{-1}.

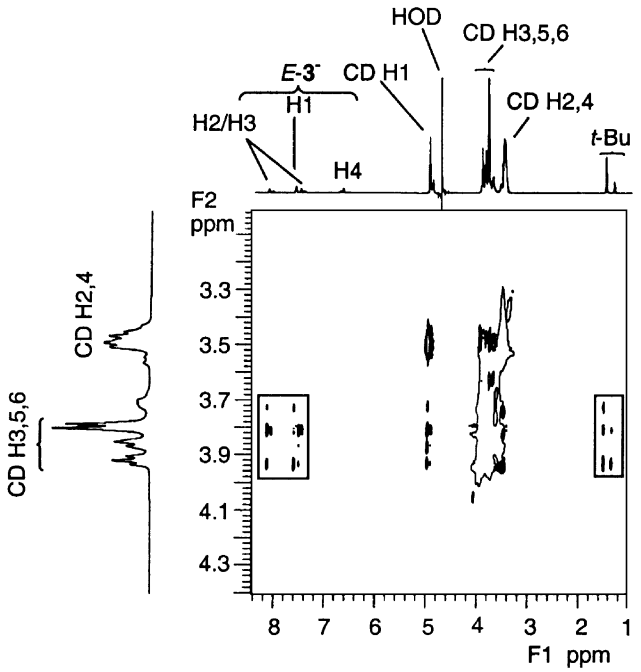

Fig. 7 ^{1}H 600 MHz ROESY NMR spectrum of 0.06 mol dm^{-3} αCD and 0.02 mol dm^{-3} *E*-**3**$^-$, which exist dominantly as (αCD)$_2$·*E*-**3**$^-$ in 0.10 mol dm^{-3} NaOD at 298 K. The cross-peaks enclosed in the rectangles correspond to NOE interactions between the protons indicated on the F1 and F2 axes.

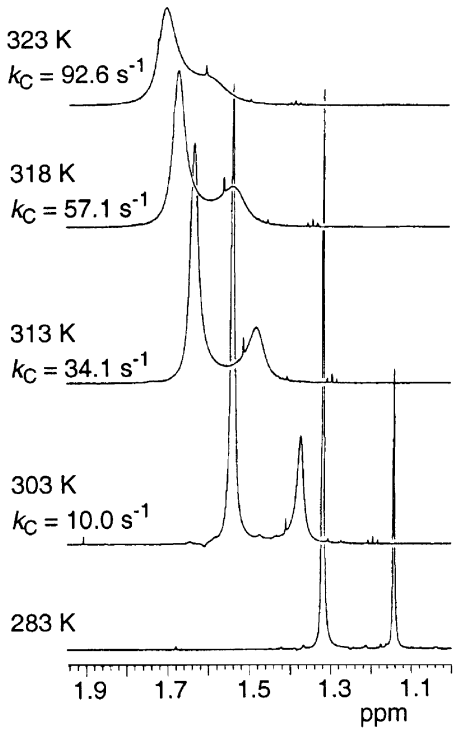

Fig. 8 Representative variable-temperature ^{1}H NMR (600 MHz) spectra of the *tert*-butyl protons of *E*-**3**$^-$ in (αCD)$_2$·*E*-**3**$^-$ showing the k_C at each temperature (k_C = 19.0 s^{-1} at 308 K and k_D = 24.6, 44.2, 75.0, 119 and 184 s^{-1} at 303, 308, 313, 318 and 323 K, respectively). The spectra are not plotted to a constant vertical scale. The solution is 0.06 mol dm^{-3} in αCD and 0.02 mol dm^{-3} in *E*-**3**$^-$ in 0.010 mol dm^{-3} NaOD.

The pairs of resonances broaden and coalesce with increase in temperature and complete lineshape analysis of the *tert*-butyl resonances in the range 303–323 K yields the kinetic parameters in Table 2, where the decomplexation rate constant, k_C, refers to includomer C (Scheme 3) and is related to k_D for includomer D through the relationship: $k_C X_C = k_D X_D$ where X_C and X_D are the mole fractions of includomers C and D, respectively. Thus, $k_C/k_{C*} = K_{21}'$ and $k_D/k_{D*} = K_{21}''$ where k_{C*} and k_{D*} are the second-order formation rate constants for includomers C and D, respectively. The aromatic *E*-**3**$^-$ protons show three pairs of doublet resonances assigned to H2–4 at 280 K and a doublet (with twice the intensity of any one of the pairs of doublets), which is attributed to the two H1 doublets possessing coincident chemical shifts in the includomers C and D (Fig. S8, ESI†). Increasing temperature causes the pairs of *E*-**3**$^-$ doublets assigned to H2 and H3 to coalesce to broad singlets at 323 K while that assigned to H4 coalesces to a doublet as the interconversion rate increases with temperature. This difference results from the greater chemical shift differences between the doublet pairs for H2 and H3 (0.079 and 0.077 ppm, respectively) and that for H4 (0.056 ppm). The coincident *E*-**3**$^-$ doublets assigned to H1 change little over the entire temperature range. These observations indicate that H1 experiences no significant difference in magnetic environment in the (αCD)$_2$·*E*-**3**$^-$ includomers while the difference in magnetic environment changes in the sequence H2 ≈ H3 > H4 for the other protons.

It has been calculated that if all motions of the CD host and the guest species ceased on going from the free state to the complexed state an entropy change of −209 to −251 J K^{-1} mol^{-1} would result.[14] On this basis the decomplexation process should have a positive entropy change of similar magnitude. This represents an upper magnitude limit for $\Delta S^{\ddagger}$ for the A and B includomers of αCD·*E*-**3**$^-$ and the C and D includomers of (αCD)$_2$·*E*-**3**$^-$ as it is unlikely that a complete cessation of motion occurs in the transition states for interconversion. The accompanying hydration changes in both the αCD and *E*-**3**$^-$ complex components occurring as the transition state is approached, particularly for the entry of water into the αCD annulus as it is partly or completely vacated by *E*-**3**$^-$, are likely to make negative entropic contributions. Changes in hydration of the *E*-**3**$^-$ 4′-oxybenzene group may also occur but their entropic contributions are not readily estimated.

Comparison may be made between the αCD·*E*-**3**$^-$ data and those for the decomplexation of αCD·**4**$^-$, where **4**$^-$ (Scheme 1) is 3,5-dimethyl-4-hydroxy-4′-sulfonatoazobenzene which is similar in size and shape to *E*-**3**$^-$ but forms a much less stable and single includomer ($K_{11} = 1.02 \times 10^3$ dm^3 mol^{-1}).[15] Both NMR and modelling studies indicate that the αCD annulus in αCD·**4**$^-$ is orientated with its narrow end toward the sulfonato group of **4**$^-$. Decomplexation occurs through a fast step followed by a slower step characterised by the parameters in Table 2. The decomplexation of the includomers of αCD·*E*-**3**$^-$ may also proceed in two steps where the slower step is that kinetically characterised by ^{1}H NMR in this study. By comparison with the slower decomplexation step for αCD·**4**$^-$, k_A(298 K) for includomer A of αCD·*E*-**3**$^-$ is 30 times greater, $\Delta H^{\ddagger}$ is larger by a factor of 1.3 and $\Delta S^{\ddagger}$ is of the same sign but 0.23 the size. For includomer B of αCD·*E*-**3**$^-$ k_A(298 K) is 87 times larger, $\Delta H^{\ddagger}$ is larger by a factor of 1.5 and $\Delta S^{\ddagger}$ is of the opposite sign and 0.25 the size $\Delta S^{\ddagger}$ of that for αCD·**4**$^-$. The most obvious differences between the **4**$^-$ and *E*-**3**$^-$ complexes are that *E*-**3**$^-$ incorporates the 4-*tert*-butylphenyl group where **4**$^-$ has a more sterically hindering 3,5-dimethyl-4-hydroxyphenyl group, and *E*-**3**$^-$ has a 4′-oxybenzene group where **4**$^-$ has a 4′-sulfonatoazobenzene group, which is likely to be more extensively hydrated. Thus, $\Delta S^{\ddagger}$ for αCD·**4**$^-$ may involve greater negative entropic contributions due to the hydration changes accompanying its decomplexation, which would explain the less negative $\Delta S^{\ddagger}$ and the positive $\Delta S^{\ddagger}$ characterising the A and B includomers of αCD·*E*-**3**$^-$, respectively. The different signs of $\Delta S^{\ddagger}$ for includomers A and B of αCD·*E*-**3**$^-$ probably reflect the opposite orientations of αCD in the includomers but further interpretation is infeasible with the present data. Greater participation of water in the approach to the transition state may offset some of the enthalpy change required to disrupt secondary bonding between αCD and **4**$^-$ as αCD·**4**$^-$ decomplexes and thereby lower the overall $\Delta H^{\ddagger}$ by comparison with those for the interconversion of the αCD·*E*-**3**$^-$ includomers.

Similar reasoning may be applied to the larger Mordant Orange 10 dianion, **5**$^{2-}$ (Scheme 1), which forms both αCD·**5**$^{2-}$ and (αCD)$_2$·**5**$^{2-}$ (characterised by $K_{11} = 1.26 \times 10^4$ dm^3 mol^{-1} and $K_{21} = 8.8 \times 10^3$ dm^3 mol^{-1}, respectively) which are 22 times less stable than αCD·*E*-**3**$^-$ and of similar stability to (αCD)$_2$·*E*-**3**$^-$, respectively.[16] The decomplexation of αCD·**5**$^{2-}$ and the decomplexation of the first αCD from (αCD)$_2$·**5**$^{2-}$ are characterised by the parameters in Table 2. By comparison with the parameters for (αCD)$_2$·**5**$^{2-}$, k_C(298 K) and k_D(298 K) for (αCD)$_2$·*E*-**3**$^-$ are 180 and 460 times greater, $\Delta H_C^{\ddagger}$ and $\Delta H_D^{\ddagger}$ are larger by factors of 1.5 and 1.3 and $\Delta S_C^{\ddagger}$ and $\Delta S_D^{\ddagger}$ are smaller by factors of 0.86 and 0.57 and are opposite in sign.

^{1}H NMR complexation studies of 1 and 2 complexes

The ^{1}H ROESY NMR spectrum of a solution equimolar in **1** and *E*-**3**$^-$ at 298 K shows cross-peaks between the αCD and βCD 3H, 5H and 6H protons and the *E*-**3**$^-$ H1–4 and *tert*-butyl protons consistent with the formation of **1**·*E*-**3**$^-$ (Fig. 9 and Scheme 2). The appearance of a cross-peak arising from the H4 proton of *E*-**3**$^-$ suggests that the urea linker between the αCD and βCD of **1** imposes a structure on **1**·*E*-**3**$^-$ which envelopes *E*-**3**$^-$ to a greater extent than is the case in (αCD)$_2$·*E*-**3**$^-$ and (βCD)$_2$·*E*-**3**$^-$. The resonances of the H1–4 protons of **1**·*E*-**3**$^-$ are greatly broadened, consistent with an exchange process occurring between different magnetic environments at an intermediate rate on the NMR timescale, whereas that of the *tert*-butyl protons is not. A possible explanation is that because of the urea linker and the homochirality of αCD and βCD each glycopyranose unit is unique such that each orientation of *E*-**3**$^-$ (with respect to the axis passing approximately through the centres of the αCD and βCD annuli of **1**) represents a rotomer of **1**·*E*-**3**$^-$ in each of which *E*-**3**$^-$ experiences different magnetic environments. Thus, rotation between the rotomer orientations

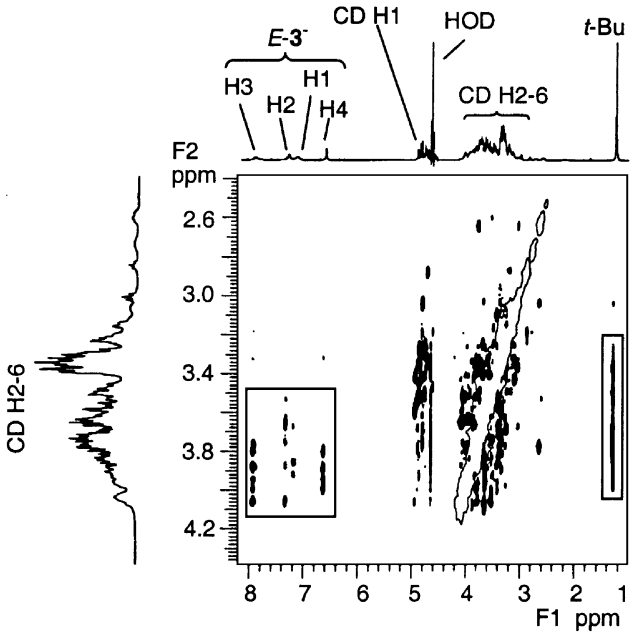

Fig. 9 ^{1}H 600 MHz ROESY NMR spectrum of 0.01 mol dm^{-3} **1** and *E*-**3**$^-$ which exist dominantly as **1**·*E*-**3**$^-$ in 0.10 mol dm^{-3} NaOD at 298 K. The cross-peaks enclosed in the rectangles correspond to NOE interactions between the protons indicated on the F1 and F2 axes.

results in broadening of the H1–4 resonances of the *E*-**3**$^-$ protons of **1**·*E*-**3**$^-$. The lack of broadening of the *tert*-butyl resonance is attributed to rapid C–C bond rotation within the *tert*-butyl group and also about the *tert*-butyl to phenyl bond resulting in a faster environmental averaging than that between the rotomers. Alternatively, a shuttling motion of *E*-**3**$^-$ along the complex axis could be the source of the resonance broadening. At 323 K the *E*-**3**$^-$ aromatic resonances of **1**·*E*-**3**$^-$ are much narrower consistent with an acceleration of the rate process.

The ^{1}H ROESY NMR spectrum of an equimolar solution of **2** and *E*-**3**$^-$ shows well-resolved doublets arising from H1-4 of *E*-**3**$^-$ with the first thee doublets showing moderately strong cross-peaks and the H4 doublet showing weaker cross-peaks with the H3, H5 and H6 protons of the βCD of **2** consistent with the formation of **2**·*E*-**3**$^-$ (Fig. 10). Again, the *tert*-butyl protons show much stronger cross-peaks commensurate with their higher population. In contrast to **1**·*E*-**3**$^-$, none of the *E*-**3**$^-$ resonances of **2**·*E*-**3**$^-$ is broadened consistent with a faster rate of either rotomerization or shuttling permitted by the looser fit of the two βCD annuli of **2** to *E*-**3**$^-$.

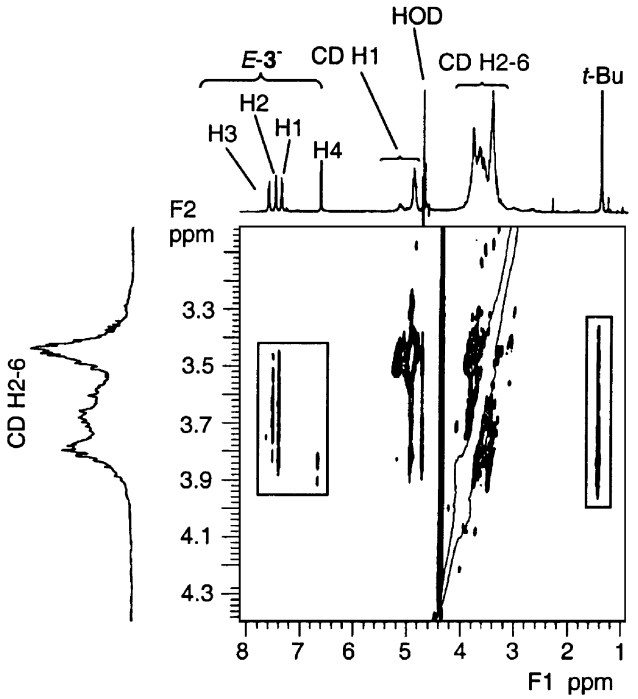

Fig. 10 ^{1}H 600 MHz ROESY NMR spectrum of 0.01 mol dm^{-3} **2** and *E*-**3**$^-$ which exist dominantly as **2**·*E*-**3**$^-$ in 0.10 mol dm^{-3} NaOD at 298 K. The cross-peaks enclosed in the rectangles correspond to NOE interactions between the protons indicated on the F1 and F2 axes.

In the presence of one equivalent of adamantane-1-carboxylate (**6**$^-$ in Scheme 1) new cross-peaks arising from the adamantyl protons and H3, H5 and H6 of the βCD components appear and the cross-peaks remain for the protons of *E*-**3**$^-$ (Fig. S9, ESI†). This is consistent with the dominant complex in solution being **2**·*E*-**3**$^-$·**6**$^-$ with the 4-*tert*-butylphenyl group of *E*-**3**$^-$ occupying one βCD annulus and **6**$^-$ the other. This suggests that the complexation of the 4-*tert*-butylphenyl group of *E*-**3**$^-$ by one βCD is a major stabilising force in **2**·*E*-**3**$^-$ with the 4′-oxybenzene group being less strongly complexed by the second βCD. As **6**$^-$ complexation by βCD[17] is characterised by K_{11} = 1.8 × 10^4 dm^3 mol^{-1} it follows that the internal complexation of the 4′-oxybenzene group in **2**·*E*-**3**$^-$ is characterised by a K_{11} less than this. (Displacement of the 4′-oxybenzene group by **6**$^-$ may involve rotation of one βCD component about the N–C(6) bond of **2** so that it is no longer approximately collinear with the second βCD component.) In contrast, a solution 0.01 mol dm^{-3} in each of **1**·*E*-**3**$^-$ and **6**$^-$ shows no cross-peaks arising from interaction of the **6**$^-$ protons with H3, H5 and H6 of the βCD of **1**. This is consistent with the complexation of the 4-*tert*-butylphenyl group of *E*-**3**$^-$ by the βCD component of **1** in **1**·*E*-**3**$^-$ and with **6**$^-$ being too large to compete effectively with the 4′-oxybenzene group of *E*-**3**$^-$ for occupancy of the annulus of the αCD component of **1**. (K_{11} = 1.4 × 10^2 dm^3 mol^{-1} for the complexation of **6**$^-$ by αCD.[17]).

The ^{1}H ROESY NMR spectrum of a solution 0.01 mol dm^{-3} in **2** and 0.02 mol dm^{-3} in *E*-**3**$^-$, which exists dominantly as **2**·(*E*-**3**$^-$)$_2$, as indicated by the UV-vis studies discussed above, shows cross-peaks very similar to those observed for **2**·*E*-**3**$^-$ (Fig. S10, ESI†).

Ab initio study of *E*-**3**$^-$

Theoretical investigations using the Gaussian 98 suite of programs[11] and the Pople-type 6-31g(d,p) basis set were undertaken to gain insight into the failure to observe *E* to *Z* (*trans* to *cis*) isomerization in **3**$^-$. Two possibilities for the lack of such isomerization were investigated: (i) while ground-state *E*-**3**$^-$ has a large isomerization barrier, that for ground-state *Z*-**3**$^-$ is very small so that *Z*-**3**$^-$ rapidly reverts to *E*-**3**$^-$, which is the only detected isomer, and as a consequence should *E*-**3**$^-$ photoisomerize to *Z*-**3**$^-$ it will rapidly revert to *E*-**3**$^-$ thermally. (ii) The first and second excited singlet electronic states of **3**$^-$, S_1 and S_2, respectively (corresponding to n–π* and π–π* transitions) have a preferred transoid conformation. Calculations at the HF/6-31g(d,p) theory level show the isomerization of *E*-**1**$^-$ to *Z*-**1**$^-$ and *vice versa* to be characterised by barriers of 183.1 and 105.9 kJ mol^{-1}, respectively. This indicates that the isomerization of *E*-**1**$^-$ to *Z*-**1** would be slow and that possibility (i) can not account for the absence of *Z*-**1**$^-$. In general terms, calculations show that the first and second excited singlet electronic states of **3**$^-$, S_1 and S_2, respectively (corresponding to n–π* and π–π* transitions) have a preferred transoid conformation which indicates that possibility (ii) is the more likely explanation for the absence of *Z*-**1**$^-$. Further discussion and details of the calculations appear as ESI.†

Experimental

General

Aqueous solutions were prepared with water purified with a Waters Milli-Q system to give a specific resistance of >15 MΩ cm which was then boiled for 30 min to remove CO_2 and allowed to cool in a container fitted with a soda lime guard tube. Sodium perchlorate (Fluka) was twice recrystallised from water, and the anhydrous salts was obtained by drying to constant weight over P_2O_5 under vacuum prior to use (**CAUTION**: Anhydrous perchlorate salts are potentially explosive and should be handled with care). UV-vis spectra of *E*-**3**$^-$ and either αCD, βCD, **1** or **2** in 0.050 mol dm^{-3} borate buffer (total buffer concentration at pH 10.0 prepared from boric acid and NaOH at I = 0.10 mol dm^{-3} adjusted with $NaClO_4$) were run at 298.2 ± 0.1 K in matched quartz cuvettes of 1 cm path length against a reference containing the same buffer and supporting electrolyte. Absorbance data were collected at 0.5 nm intervals with a Cary 300 Bio double beam spectrophotometer.

Complex stoichiometry and complexation constants were determined through non-linear least squares fitting of algorithms for the formation of 1 : 1, 1 : 1 and 2 : 1, 1 : 2, and 2 : 1 complexes to the absorbance variation of *E*-**3**$^-$ with concentration of αCD, βCD, **1** and **2** at 1 nm intervals in the range 350–500 nm by using Method 5 of Pitha and Jones,[18] through a least-squares regression routine DATAFIT[19] using the MATLAB formalism.[20] Using the αCD/*E*-**3**$^-$ system as an example, the observed absorbance, A, is related to the molar absorbances of the species in solution, ε, and their concentrations through:

$$A = \varepsilon_{\alpha CD}[\alpha CD] + \varepsilon_{E\text{-}3}[E\text{-}3^-] + \varepsilon_{\alpha CD\cdot E\text{-}3}[\alpha CD\cdot E\text{-}3^-] + \varepsilon_{(\alpha CD)_2\cdot E\text{-}3}[(\alpha CD)_2\cdot E\text{-}3^-] \quad (1)$$

where $\varepsilon_{\alpha CD} = 0$ and species concentrations are related through the complexation constants $K_{11} = [\alpha CD{\cdot}E\text{-}\mathbf{3}^-]/([\alpha CD][E\text{-}\mathbf{3}^-])$ and $K_{21} = [(\alpha CD)_2{\cdot}E\text{-}\mathbf{3}^-]/([\alpha CD][\alpha CD{\cdot}E\text{-}\mathbf{3}^-])$.

^{1}H (600 MHz) and ^{13}C (75.5 MHz) NMR spectra were run on Inova 600 and Varian Gemini 300 spectrometers, respectively. Solutions of E-**3**$^-$ and either αCD, βCD, **1** or **2** were prepared from E-**3**H in 0.10 mol dm^{-3} NaOD in D_2O and had a pD ≈ 12. Chemical shifts were referenced against external trimethylsilylpropiosulfonic acid. Elemental analyses were performed by the Microanalytical Service of the Chemistry Department, University of Otago, Dunedin, New Zealand. αCD and βCD (Nihon Shokhuin Kako Co.) were dried by heating at 100 °C under vacuum for 18 h.

Syntheses

N-(6^A-Deoxy-α-cyclodextrin-6^A-yl)-*N*′-(6^A-deoxy-β-cyclodextrin-6^A-yl)urea (**1**) and *N*,*N*-bis(6^A-deoxy-β-cyclodextrin-6^A-yl)urea (**2**) were prepared as in the literature and gave spectroscopic data in good agreement with those reported.[1,2]

4-*tert*-Butyl-4′-hydroxyazobenzene (*E*-3H)

A cold solution of sodium nitrite (BDH, 560 mg, 8.11 mmol) in water (5 cm^3) was added dropwise to a vigorously stirred solution of 4-*tert*-butylaniline (Aldrich, 800 mg, 5.37 mmol) in concentrated aqueous hydrochloric acid (Ajax Univar, 3 cm^3) and water (3 cm^3) cooled in an ice-salt-bath, at such a rate that the temperature of the mixture did not exceed 0 °C. The resultant solution was stirred for a further 5 min at 0 °C and then added dropwise to a stirred solution of phenol (Aldrich, 860 mg, 9.15 mmol) in 10% aqueous sodium hydroxide (Ajax Univar, 10 cm^3) cooled to 0 °C. The reaction mixture was left to stir at 0 °C for 30 min and the crude product was collected by vacuum filtration and washed with water. The product was recrystallised from aqueous ethanol as yellow–orange needles (1.18 g, 87%); mp 124–126 °C. Elemental analysis for $C_{16}H_{18}N_2O{\cdot}0.5H_2O$: C, 72.98; H, 7.27; N, 10.64. Found C, 73.38; H, 7.32; N, 10.85%. δ_H ($CDCl_3$) 8.83 (d, J = 8.4 Hz, 2H), 7.80 (d, J = 8.4 Hz, 2H), 7.51 (d, J = 8.4 Hz, 2H), 6.90 (d, J = 8.4 Hz, 2H), 1.36 (s, 9H). δ_C ($CDCl_3$) 158.1, 154.0, 150.6, 147.2, 126.0, 124.8, 122.2, 115.8, 31.2.

Acknowledgements

We thank the Australian Research Council and the University of Adelaide for supporting this research, and for Nihon Shokhuin Kako Co. Ltd. for a gift of β-cyclodextrin.

References

1 M. M. Cieslinski, P. Clements, B. L. May, C. J. Easton and S. F. Lincoln, *J. Chem. Soc., Perkin Trans. 2*, 2002, 947 (in this reference the concentration scales of Fig. 2(a) and (b) should read $10^3[\mathbf{1}]_{total}$/mol dm^{-3} and $10^3[\mathbf{2}]_{total}$/mol dm^{-3}, respectively).
2 C. J. Easton, S. J. van Eyk, S. F. Lincoln, B. L. May, J. Papageorgiou and M. L. Williams, *Aust. J. Chem*, 1997, **50**, 9.
3 D. B. Amabilino and J. F. Stoddart, *Chem. Rev.*, 1995, **95**, 2725; C. J. Easton and S. F. Lincoln, *Chem. Soc. Rev.*, 1996, **25**, 163; K. A. Connors, *Chem. Rev.*, 1997, **97**, 1325; H. J. Schneider, F. Hacket, V. Rüdiger and H. Ikeda, *Chem. Rev.*, 1998, **98**, 1775; M. V. Rekharsky and Y. Inoue, *Chem. Rev.*, 1998, **98**, 1875.
4 C. J. Easton and S. F. Lincoln, *Modified Cyclodextrins, Scaffolds and Templates for Supramolecular Chemistry*, Imperial College Press, London, UK, 1999.
5 C. A. Haskard, C. J. Easton, B. L. May and S. F. Lincoln, *J. Phys. Chem.*, 1996, **100**, 14457.
6 C. A. Haskard, B. L. May, T. Kurucsev, S. F. Lincoln and C. J. Easton, *J. Chem. Soc., Faraday Trans.*, 1997, **93**, 279.
7 P. Cattaneo and M. Perisco, *Phys. Chem. Chem. Phys*, 1999, **1**, 4739.
8 T. Ishikawa, T. Noro and T. Shoda, *J. Chem. Phys.*, 2001, **115**, 7503.
9 Y. Hirose, H. Hiroharu and T. Sawada, *J. Phys. Chem. A*, 2002, **106**, 3067.
10 T. Fujino, S. Y. Arzhantzev and Y. Tahara, *Bull. Chem. Soc. Jpn.*, 2002, **75**, 1031.
11 *Gaussian 98, Revision A.11.3*, M. J. Frisch, G. W. Trucks, H. B. Schlegel, G. E. Scuseria, M. A. Robb, J. R. Cheeseman, V. G. Zakrzewski, J. A. Montgomery, R. E. Stratmann, J. C. Burant, S. Dapprich, J. M. Millam, A. D. Daniels, K. N. Kudin, M. C. Strain, O. Farkas, J. Tomasi, V. Barone, M. Cossi, R. Cammi, B. Mennucci, C. Pomelli, C. Adamo, S. Clifford, J. Ochterski, G. A. Petersson, P. Y. Ayala, Q. Cui, K. Morokuma, N. Rega, P. Salvador, J. J. Dannenberg, D. K. Malick, A. D. Rabuck, K. Raghavachari, J. B. Foresman, J. Cioslowski, J. V. Ortiz, A. G. Baboul, B. B. Stefanov, G. Liu, A. Liashenko, P. Piskorz, I. Komaromi, R. Gomperts, R. L. Martin, D. J. Fox, T. Keith, M. A. Al-Laham, C. Y. Peng, A. Nanayakkara, M. Challacombe, P. M. W. Gill, B. Johnson, W. Chen, M. W. Wong, J. L. Andres, C. Gonzalez, M. Head-Gordon, E. S. Replogle, J. A. Pople, Gaussian, Inc., Pittsburgh PA, 2002.
12 S. F. Lincoln, *Prog. React. Kinet.*, 1977, **9**, 1.
13 Program *DAVTNMR*: personal communication from David Brittain, University of Adelaide, 2003; I. Tabushi, Y.-I. Kiyosuke, T. Sugimoto and K. Yamamura, *J. Am. Chem. Soc.*, 1978, **100**, 916.
14 A. Abou-Hamdan, P. Bugnon, C. Saudan, P. G. Lye and A. E. Merbach, *J. Am. Chem. Soc.*, 2000, **122**, 592.
15 C. Saudan, F. A. Dunand, A. Abou-Hamdan, P. Bugnon, P. G. Lye, S. F. Lincoln and A. E. Merbach, *J. Am. Chem. Soc.*, 2001, **123**, 10290.
16 M. R. Eftink, M. L. Andy, K. Bystrom, H. D. Perlmutter and D. S. Kristol, *J. Am. Chem. Soc.*, 1989, **111**, 6765.
17 J. Pitha and R. N. Jones, *Can. J. Chem.*, 1966, **44**, 1303.
18 *DATAFIT*: T. Kurucsev, University of Adelaide, 1988.
19 *MATLAB 4.2b*: The MathWorks, Inc., Cochituate Place, 24 Prime Park Way, Natick, MA, 01760, USA.